A LARGE SIGNAL NONLINEAR MODFET MODEL FROM SMALL SIGNAL S-PARAMETERS[*]

J. M. O'Callaghan and J. B. Beyer

University of Wisconsin-Madison
Department of Electrical and Computer Engineering
1415 Johnson Drive, Madison, WI   53706-1691

ABSTRACT

A general technique for predicting the FET large signal performance has been developed. The technique is based entirely on experimental data (small signal S-parameters at different bias points) and therefore is independent of the structure of the FET. Large signal measurements confirm the validity of the model.

I. INTRODUCTION

Modulation doped FETs (MODFETS) have already been proven to have good noise performance for microwave applications (1). MODFETs are also well suited for class B amplifiers, since their transfer characteristic can be approximated by a piecewise linear curve and this leads to a large signal transconductance independent of the signal level. However, there are few large signal models available and the determination of the parameters of such models is difficult or requires special equipment. Furthermore, the models cannot be used conveniently in common CAD programs.

The model and measurement techniques presented here overcome these problems. Software requirements include: a program (like TOUCHSTONE™) to fit an equivalent circuit to S parameter data; a simple least square polynomial approximation program; and the popular SPICE for nonlinear time domain simulations. Hardware requirements are basically limited to a network analyzer to carry out the small signal S parameter measurements.

II. NONLINEAR MODFET CIRCUIT MODEL

A. Circuit Elements

The nonlinear circuit proposed is an extension of a widely used small signal equivalent circuit in which the nonlinearity of $C_{gs}(v_1)$ and $I_{ds}(v_1,v_{ds})$ is taken into account (see Fig. 1). In this circuit $I_{ds}(v_1,v_{ds})$ models the nonlinearities of the transconductance (g_m) and the output conductance (G_0) through Eqs. 1 and 2:

$$G_0(v_1,v_{ds}) = \frac{\partial I_{ds}(v_1,v_{ds})}{\partial v_{ds}} \qquad (1)$$

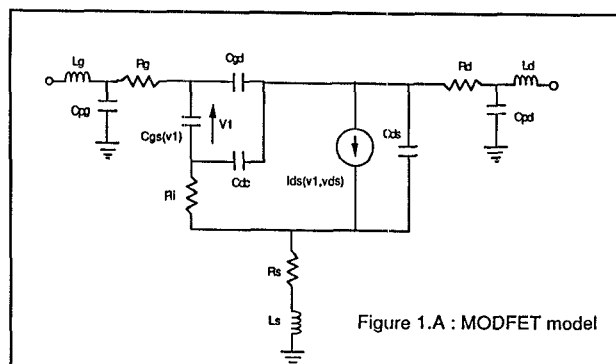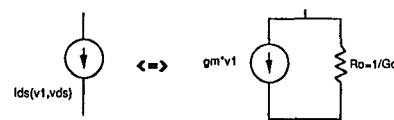$$g_m(v_1,v_{ds}) = \frac{\partial I_{ds}(v_1,v_{ds})}{\partial v_1} \qquad (2)$$

Figure 1.A : MODFET model

Figure 1.B : Small signal equivalent of Ids

B. Determination of the Linear Element Values

The values of C_{ds} and the extrinsic elements have been determined for a 300µm SONY MODFET by measuring its S parameters at $V_{DS},V_{GS} = 0$ and fitting its equivalent circuit at this bias point (Fig. 2) (2), (3) (See Table 1). In our model, only C_{gs} and I_{ds} are allowed to be voltage-dependent. To describe this dependence we have to adjust g_m, G_0, C_{gs}, R_i, C_{gd} and C_{dc} in Fig. 1 to match the S parameters at several bias points. Only the first three parameters are used to characterize the nonlinear behavior of $C_{gs}(v_1)$ and $I_{ds}(v_1,v_{ds})$(4). The linearized equivalents of R_i, C_{gd}, and C_{dc} are found by averaging their values at these bias points. The obtained values are:

$R_i = 1.22\ \Omega; \quad C_{gd} = 0.0438\ pF; \quad C_{dc} = 0.0518\ pF$
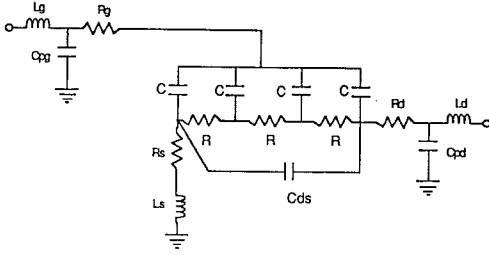

Figure 2 Zero-bias equivalent circuit

Table 1: Linear elements from zero bias circuit

$L_d = 0.0741\ nH$ $L_g = 0.0478\ nH$ $L_s = 0.0588\ nH$

$R_d = 1.39\ \Omega$ $R_g = 1.36\ \Omega$ $R_s = 1.22\ \Omega$

$C_{ds} = 0.0219\ pF$ $C_{pg} = 0.0267\ pF$ $C_{pd} = 0.0371\ pF$

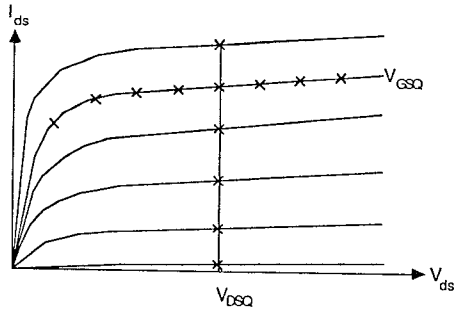## C. Determination of $Ids(v_1, v_{ds})$

Figure 3 Distribution of the bias points

Figure 3 shows the distribution of the bias points for which a small signal equivalent circuit has been determined. If we assume that $Ids(v_1, v_{ds})$ can be expressed as a product of two one-variable functions; i.e.:

$$I_{ds}(v_1, v_{ds}) = p_g(v_1)p_d(v_{ds}) \qquad (3)$$

$p_g(v_1)$ can be found from the transfer function at $v_{ds} = V_{DSQ}$:

$$p_g(v_1) = \frac{I_{ds}(v_1, V_{DSQ})}{p_d(V_{DSQ})} \qquad (4)$$

At this point we can set $pd(V_{DSQ}) = 1$; then $p_g(v_1)$ is forced to take the values of the transfer characteristic. From Eq. 2 and knowing that

$$I_{ds}(V_T, V_{DSQ}) = 0 \qquad (5)$$

(V_T being the pinch-off voltage), we can write

$$p_g(v_1) = \int_{V_T}^{v_1} g_m(u, V_{DSQ})du \qquad (6)$$

which allows us to evaluate the v_1 dependence of I_{ds} from the measured g_m at several bias points. Figure 4 shows the values of g_m measured for V_{GS} ranging from -1.4V to 0.4V and $V_{DS} = V_{DSQ} = 2V$ and their corresponding values of p_g (or $Ids(v_1, V_{DSQ})$) found with Eq. 6.

Similar steps are taken to determine the dependence of I_{ds} with v_{ds}: from Eqs. 1 and 3 we know that

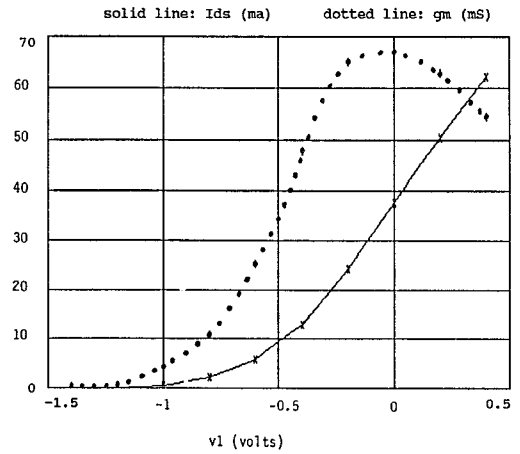$$G_0(V_{GSQ}, v_{ds}) = p_g(V_{GSQ})p_d'(v_{ds}) \qquad (7)$$

FIGURE 4:   TRANSCONDUCTANCE AND TRANSFER CURVE FOR Vds=VDSQ=2V

but $p_g(V_{GSQ}) = I_{ds}(V_{GSQ}, V_{DSQ})$ so

$$p_d'(v_{ds}) = \frac{G_0(V_{GSQ}, v_{ds})}{I_{ds}(V_{GSQ}, V_{DSQ})} \qquad (8)$$

This equation, with the condition $p_d(V_{DSQ}) = 1$ leads to p_d for the nonzero values of v_{ds}:

$$p_d(v_{ds}) = 1 + \frac{1}{I_{ds}(V_{GSQ}, V_{DSQ})} \int_{V_{DSQ}}^{v_{ds}} G_0(V_{GSQ}, u)du \qquad (9)$$

Also, since $I_{ds}(v_1, 0) = 0$, p_d has to be zero for $v_{ds} = 0$.

In Table 2, the practical application of Eq. 9 is shown: Starting from the values of $G_0(V_{GSQ}, V_{DS})$ and performing the numerical integration indicated in Eq. 9, the values of $p_d(V_{DS})$ are found for V_{DS} ranging from 0.5 to 4V.

D. Polynomial fitting of $p_g(v_1)$, $p_d(v_{ds})$ and $C_{gs}(v_1)$ for class B applications

The approach discussed so far has allowed us to describe the voltage dependencies with one-variable functions. What is needed now is to express these functions in a form that can be

Table 2 - Determination of $P_d(V_{DS})$ from Output Conductance Data ($V_{GS} = V_{GSQ} = -0.2V$)

V_{DS}	0.5	1.0	2.0	3.0	4.0
G_0 (mS)	18.9751	8.2583	5.2548	3.7447	3.4330
$\int_{V_{DSQ}}^{V_{DS}} G_0$ (mA)	-13.5647	-6.7563	0	4.4995	8.0884
$P_d(V_{DS})$	0.4408	0.7215	1	1.1855	1.3334

handled by a CAD program. Our work has been focused towards getting a model for SPICE, whose user-defined nonlinearities have to be expressed in polynomial form.

There are several methods to fit a polynomial to a set of data. Our choice is the one described by Hayes (5) in which the sum of the squares of the residual error is minimized by using a sum of orthogonal polynomials. Other algorithms as well as commericial software can be used for this purpose.

For simulating class A operation we need to get data at $V_T < v_1 < v_{max}$ and carry out the fitting of $p_g(v_1)$ and $C_{gs}(v_1)$ in this range. However, for class B and C operation it might not be necessary to take measurements in the whole range of values of v_1. This is because we know beforehand that $p_g(0) = 0$ for $v_1 < V_T$ and that $C_{gs}(v_1)$ behaves smoothly in this range. Advantage is taken of both facts to limit the measurement range to $V_T < v_1 < v_{1max}$. In our case we are interested in class B operation and our device has $V_T = -1V$ and $v_{1max} = 0.4V$ which makes our class B range $-2.4 \leq v_1 \leq 0.4$.

Extrapolation of p_g below the pinch-off voltage consists of adding zeros at discrete values of v_1. Figure 5 shows the process for our particular case (5.4μA rms error with a 10 degree polynomial).

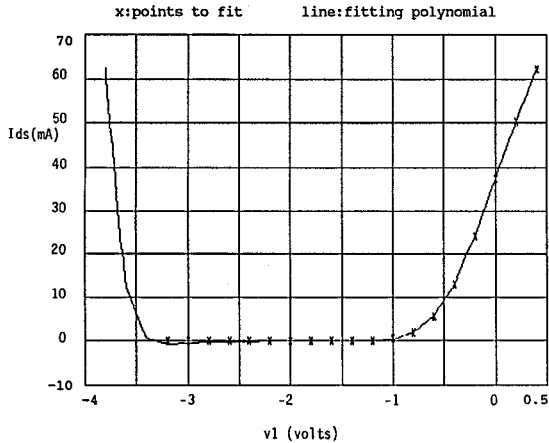x:points to fit   line:fitting polynomial

FIGURE 5:   POLYNOMIAL FITTING OF THE TRANSFER CURVE

Note that for the lower values of v_1, $p_g(v_1)$ is quite different from zero. This is a typical characteristic of polynomial fitting, i.e. the (absolute) error tends to be higher at the extremes of the fitting interval. Therefore, we can expect to have the highest relative errors at the leftmost extreme of the transfer characteristic where the currents are small but the fitting error can be high. To avoid this effect, a few zeros were added at values of v_1 less than -2.4V.

Extrapolation of $C_{gs}(v_1)$ is more involved. First, a coefficient m has to be found to fit the measured values of C_{gs} to the expression

$$C_{gs}(v_1) = \frac{C_{gs}(0)}{(1 - \frac{v_1}{0.8})^m} \qquad (10)$$

which can be later used to find C_{gs} for $v_1 < V_T$. Figure 6 summarizes this process for our particular case ($m = 0.474$). A 3.8 fF rms error is obtained with an 8 degree polynomial.
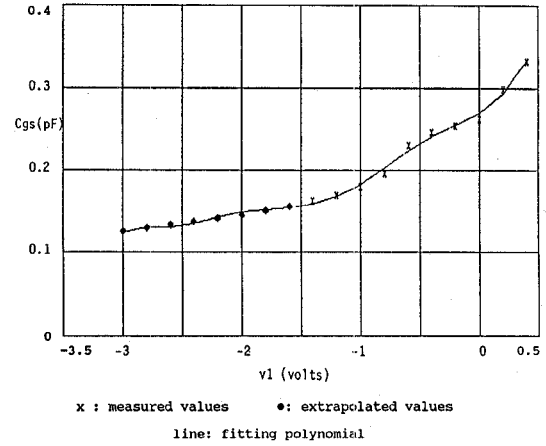

x : measured values   •: extrapolated values

line: fitting polynomial

FIGURE 6:   POLYNOMIAL FITTING OF $C_{gs}(v1)$ AT Vds=VDSQ=2V

Finally, $p_d(v_{ds})$ has to be interpolated to the values shown in Table 2 and the point $P_d(0) = 0$. Note that since interpolation is a particular case of polynomial fitting, the same software that has been used to fit $p_g(v_1)$ and $C_{gs}(v_1)$ can now be used to interpolate $p_d(v_{ds})$.

III. EXPERIMENTAL RESULTS

Measurements at 10 GHz on a SONY MODFET 2SK677H5 were made to confirm the three basic nonlinear effects:

● Nonlinearity in C_{gs}

● Nonlinear dependence of Ids with v_{ds}

● Nonlinear dependence of Ids with v_1

The accuracy of the nonlinear behavior of $C_{gs}(v_1)$ was checked by measuring the large signal S_{11} and comparing it with simulated data. This is shown in Figure 7, where the measured class A and class B S_{11} are compared to the calculated ones for two values of incident power.
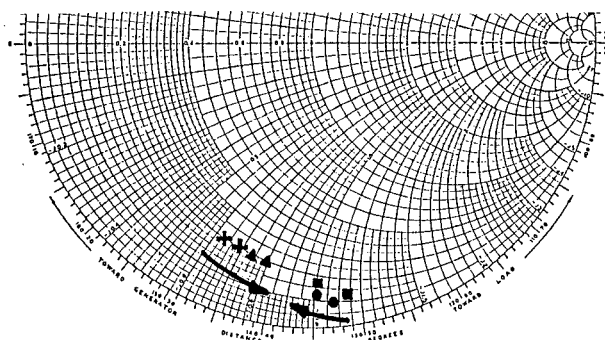
349

FIGURE 7: LARGE SIGNAL S11

+ Measured Class A⎫ V$_{DS}$ = 3V   V$_{GS}$ = -0.31V
▲ Simulated Class A⎭ P$_{IN\ min}$ = -5.86 dBm P$_{IN\ max}$ = 6.64 dBm

● Measured Class B⎫ V$_{DS}$ = 3V   V$_{GS}$ = -1V
■ Simulated Class B⎭ P$_{IN\ min}$ = -5.86 dBm P$_{IN\ max}$ = 9.14 dBm

-The arrows indicate the change in S11 with increasing P$_{IN}$

Current in mA   x: measured   solid line:calculated

Power incident in dBm

FIGURE 9: DC CURRENT GENERATED IN CLASS B OPERATION

Similarly, the large signal S_{22} is expected to be sensitive to the nonlinear dependence of I_{ds} with v_{ds}. Figure 8 shows comparitive results of this parameter at two bias levels. (This parameter showed low sensitivity to the incident power).
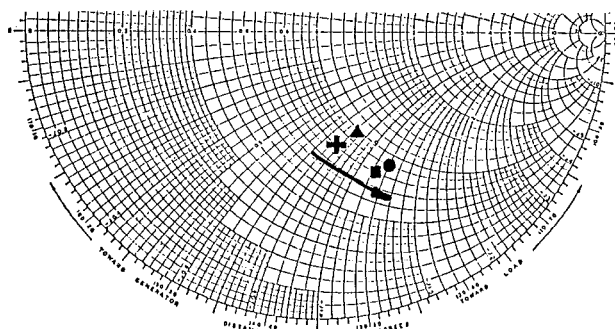

FIGURE 8: LARGE SIGNAL S22

✛ Measured ⎫ V$_{DS}$ = 1V ; V$_{GS}$ = -0.31V
▲ Simulated ⎭

● Measured ⎫ V$_{DS}$ = 3V ; V$_{GS}$ = -0.31V
■ Simulated ⎭

-Incident Power: P$_{IN}$ = 4.14dBm
-The arrow indicates the change in S22 with increasing V$_{DS}$

Finally, the accuracy in the modeled transfer characteristic was checked by comparing the measured DC current generated in class B operation to the calculated value. This is shown in Figure 9 and again, good agreement is found.

IV. CONCLUSIONS

FET modeling can be done with little hardware and common software. The proposed model does not make any assumption as to the physical structure of the FET, and the CAD simulations are in good agreement with large signal measurements.
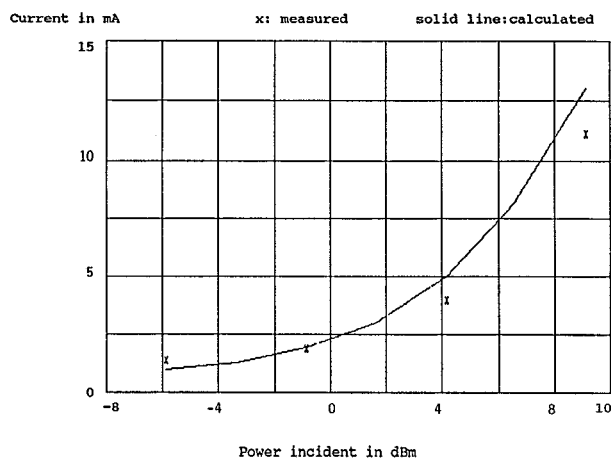
V. REFERENCES

(1) K. Josin, T. Mimura, Y. Yamashita, K. Kosemura and T. Saito, "Noise Performance of Microwave HEMT," IEEE MTT-S Int. Symp. Dig. June 1983.

(2) W. Curtice, "GaAs MESFET Modeling and Nonlinear CAD," IEEE T-MTT, February 1988.

(3) F. Diamond and M. Laviron, "Measurement of Extrinsic Series Elements of a Microwave FET Under Zero Current Conditions," Proc. 12th European Microwave Conference (Finland), September 1982.

(4) C. Rausher and H. A. Willing, "Simulation of Nonlinear FET Performance Using a Quasi-Static Model," IEEE T-MTT, October 1979.

(5) J. C. Hayes, Editor, "Numerical Approximation to Functions and Data," Athlone Press, 1970.